

Confounding effects of imaging gradients in stimulated echo: case of diffusion exchange imaging

Samo Lasic¹, Henrik Lundell², Casper Kaae Sønderby², Daniel Topgaard³, and Tim B. Dyrby²

¹CR Development, Lund, Skåne, Sweden, ²Danish Research Centre for Magnetic Resonance, Copenhagen University Hospital, Hvidovre, Denmark, ³Physical Chemistry, Lund University, Lund, Skåne, Sweden

Introduction: Diffusion-weighted stimulated echo (STE) sequences are often used in applications where T2 is short compared to the diffusion times, e.g. at higher fields. The STE is also common in diffusion correlation experiments such as double pulsed field gradient (dPFG) used to measure diffusional exchange¹⁻³ or angular dPFG to measure microscopic anisotropy⁴. In a STE pulse sequence, slice gradients as well as crusher gradients⁵ (together known as butterfly gradients) introduce additional diffusion weighting⁶. The butterfly gradients may significantly disrupt the experimental design, for example when STE is used in high angular resolution diffusion imaging experiments with single diffusion encoding, but in this case the effects of butterfly gradients can be easily compensated⁶. On the other hand, in experiments that rely on varying the mixing time, t_m , during which diffusion weighting is not desired, such as in filter exchange imaging (FEXI)^{2,3,7}, the butterfly gradients may introduce a bias that cannot be easily mitigated. Here we discuss the bias caused by butterfly gradients used in FEXI and their possible confounding effect on the measurement of apparent exchange rate (AXR).

Methods: Fresh beaker's yeast mixed with tap water (3:1 weight ratio) was measured at room temperature on a preclinical Agilent 4.7 T MRI scanner similar as in ⁷. FEXI (Fig. 1A) was performed with: TR = 2.5 s, $\delta/\Delta = 5/10$ ms, 7 t_m between 10 and 300 ms, diffusion weighting of the filter block, $b_f = 0$, 2381 s/mm² and detection block, $b = 45, 50, 61, 93, 192, 489$ and 1387 s/mm². 1 ms long crusher gradient was applied with increasing gradient strengths in 8 steps from 0 to 400 mT/m. Three 3 mm slices were excited with sinc modulated radio frequency (RF) pulses ($\delta_s = 2$ ms) with spectral width, $sw_h = 2972$ Hz. ADC(t_m) shown in Fig. 1B was analyzed based on the signal from the middle slice of the entire sample region.

Synthetic data was generated using a two-site exchange model⁸. The values shown in Fig. 1C were obtained by the standard AXR analysis^{2,3,7}. The signal evolution for FEXI can be decomposed in three steps corresponding to the filter, mixing and detection blocks^{2,3,7}. The evolution of the signal contributions from sites 1 and 2, $\mathbf{S}^T = (S_1, S_2)$, is given by

$$\mathbf{S} = S_0 \exp(-b\mathbf{D} + \mathbf{K}t_d) \cdot \exp[-(2\pi q_b)^2 \mathbf{D} + \mathbf{K}] t_m] \cdot \exp(-b_f \mathbf{D} + \mathbf{K}t_f) \cdot \mathbf{f}, \quad \text{Eq. 1}$$

where q_b denotes the unwanted dephasing⁵ due to butterfly gradients, $t_d = \Delta - \delta/3$ (see Fig. 1A), $\mathbf{f}^T = (f_1, f_2)$ are the equilibrium fractions of the signals from the two sites and S_0 is the normalization factor. The exchange and diffusion matrices are defined as

$$\mathbf{K} = \begin{pmatrix} -k_{12} & k_{21} \\ k_{12} & -k_{21} \end{pmatrix} \text{ and } \mathbf{D} = \begin{pmatrix} D_1 & 0 \\ 0 & D_2 \end{pmatrix}, \text{ respectively, where } k_{12} \text{ and } k_{21}$$

are the forward/backward exchange rates between sites 1 and 2 and $D_{1,2}$ are the diffusivities in the respective sites.

Assuming a minimum phase of 4π is required to eliminate additional echoes by the crusher gradient⁵, the dephasing due to the butterfly gradients (crusher and slice select) is, for a slice thickness dz , given by

$$q_b = 4\pi/dz + \pi sw_h \delta_s/dz, \quad \text{Eq. 2}$$

where sw_h is the spectral width of the RF pulse and δ_s is the duration of the slice gradient.

Results: In FEXI (Fig. 1A), the diffusion weighting due to the butterfly gradients, provides for an extended diffusion filtering effect, resulting in a modulation of ADC as a function of t_m during the mixing block. The effect is exemplified by the FEXI data acquired on the yeast phantom (Fig. 1B). By increasing the crusher gradient, the filtered (solid lines) and non-filtered ADC (dashed lines) converge to a value that is reduced compared to the equilibrium ADC at $t_m = 0$. The effect of the unwanted diffusion weighting is more pronounced at low exchange rates, $k = k_{12} + k_{21}$, which can be interpreted as the filter efficiency being reduced at higher k . The effect can also be inferred from the simulated data shown in Fig. 1C, where the AXR/ k bias is examined as a function of slice thickness. For reduced slice thickness, the unwanted diffusion weighting due to the butterfly gradients increases leading to increasingly underestimated AXR values, which is less prominent at higher exchange rates, k (compare blue and red lines).

Discussion: The confounding effect of butterfly gradients is demonstrated for the case of FEXI, but it may apply also to other experiments using STE. Effects resembling the reduced asymptotic ADC value, as seen in Fig. 1B, may be a consequence of sites with distinctly different exchange rates, where a slow exchange component cannot be detected during t_m ^{3,7}. When interpreting FEXI results, it is therefore important to examine the effect of butterfly gradients. Due to the butterfly gradients in FEXI, reducing the slice thickness inevitably leads to increased diffusion weighting during t_m , hence resulting in an AXR bias. The effect of butterfly gradients may potentially disrupt the experimental design and should be considered when using STE in multiple diffusion encoding sequences. A compensation scheme, as the one we presented for the DTI STE sequence⁶, cannot be used in this situation. Alternative sequence design modifications allowing to circumvent or account for the confounding effects of butterfly gradients would therefore be of great importance in dPFG experiments.

References: 1. Callaghan, P. T. & Fúró, I. Diffusion-diffusion correlation and exchange as a signature for local order and dynamics. *J. Chem. Phys.* **120**, 4032–4038 (2004). 2. Lasić, S., Nilsson, M., Lätt, J., Ståhlberg, F. & Topgaard, D. Apparent exchange rate mapping with diffusion MRI. *Magn. Reson. Med.* **66**, 356–365 (2011). 3. Nilsson, M. *et al.* Noninvasive mapping of water diffusional exchange in the human brain using filter-exchange imaging. *Magn. Reson. Med.* **69**, 1572–80 (2013). 4. Shemesh, N. & Cohen, Y. Microscopic and compartment shape anisotropies in gray and white matter revealed by angular bipolar double-PFG MR. *Magn. Reson. Med.* **65**, 1216–27 (2011). 5. Bernstein, M., King, K. & Zhou, X. *Handbook of MRI Pulse Sequences. Handb. MRI Pulse Seq.* 292–362 (Elsevier, 2004). 6. Lundell, H., Alexander, D. C. & Dyrby, T. B. High angular resolution diffusion imaging with stimulated echoes: compensation and correction in experiment design and analysis. *NMR Biomed.* (2014). 7. Sønderby, C. K., Lundell, H. M., Søgaard, L. V. & Dyrby, T. B. Apparent exchange rate imaging in anisotropic systems. *Magn. Reson. Med.* **72**, 756–762 (2014). 8. Kärger, J. NMR self-diffusion studies in heterogeneous systems. *Adv. Colloid Interface Sci.* **23**, 129–148 (1985).

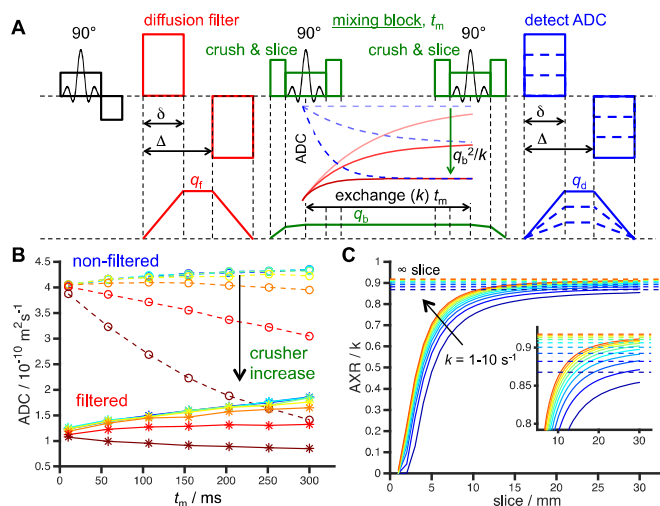


Figure 1 Effects of butterfly gradients in FEXI. A. FEXI pulse sequence with effective diffusion gradients and the corresponding dephasing for the filter, q_f (red), and detection, q_d (blue), blocks. The butterfly gradients and their dephasing, q_b , during t_m are shown in green. B. Experimental results from yeast suspension show ADC(t_m) for non-filtered ($b_f = 0$, dashed lines) and filtered (solid lines) experiments for increasing strength of the crusher gradients (blue, green to red). C. Results of fitting the AXR model to the synthetic data generated using Eq. 1. Shown is the ratio AXR/ k as a function of the slice thickness assuming a minimum dephasing, q_b , according to Eq. 2.